

UDC 541.1, 5367, 621.794

PACS numbers: 75.75.Cd, 76.80.+y

doi: 10.15330/jpnu.3.1.29-37

## THE EFFECT OF $\text{SO}_4^{2-}$ SULPHATE ANIONS ON THE ULTRAFINE TITANIA NUCLEATION

V.O. KOTSYUBYNSKY, I.F. MYRONYUK, B.K. OSTAFIYCHUK, V.L. CHELYADYN,

A.B. HRUBIAK, I.I. HRYHORUK

**Abstract.** We have proposed and experimentally tested a phenomenological model of  $\text{SO}_4^{2-}$  sulphate anions effect on the titania nucleation during hydrolysis of titanium tetrachloride. Sulphate anions form the chelating bidentate complexes with primary  $[\text{Ti}(\text{OH})_h(\text{OH}_2)_{6-h}]^{(4-h)+}$  with the influence on the next olation process and promotion of anatase phase nucleation.

**Keywords:** hydrolysis, polycondensation, nucleation, anatase, sulphate anions.

### 1. INTRODUCTION

Ultrafine  $\text{TiO}_2$  has wide range of highly promising applications in many different fields – from environmental oriented photocatalytic system (degradation of hazardous organic compound [1], waste water cleaning [2], direct decomposition of  $\text{NO}_x$ ,  $\text{SO}_x$  and air purification [3] to novel fields of industry (sensor materials [4], solar energy cells [5]). For all cases phase composition, particles size and state of surface are the most important characteristics which will determine catalytic reactivity, photosensitivity and adsorption properties of  $\text{TiO}_2$ . For example the decrease of particle size of titania leads to the catalytic activity rapidly increasing [6]. At the same time the photocatalyst properties are very sensitive to phase composition (the ratio of  $\text{TiO}_2$  polymorphs – anatase, brookite and rutile) [7]. As a result the choice of titania synthesis method with the precisiuous control of its physicochemical parameters is the crucially important. The preparation of nanosized  $\text{TiO}_2$  is possible with the using of different techniques. There are some different methods: Sol–gel [8], chemical precipitation [9], microemulsion [8], hydrothermal [10]. Sol–gel method is the most flexible techniques, temperature for nanosized oxide preparation. The variations of primary precursor types, hydrolysis conditions, temperature and pH reaction medium open the possibility to control nanocrystalline products nucleation and growth. Sol–gel method of titania obtaining typically is based on the the reactions of titanium alkoxides  $\text{Ti}(\text{OR})_n$  hydrolysis. The changing of these expensive chemicals on the cheaper precursor such as  $\text{TiCl}_4$  is very promising for nanosized large scale manufacturing by soft chemical technique. Promising advantage of  $\text{TiCl}_4$  hydrolysis is the possibility of additional control for sol-gel process polycondensation stage by using of additive ions in the reaction medium that leads to predicted nucleation of titania polymorphs specified phase. The aim of this paper is an investigation the effect of  $\text{SO}_4^{2-}$  sulphate anions on

oligomers polycondensation and oxide network formation stages of the titania nucleation during based on  $\text{TiCl}_4$  hydrolysis sol-gel process.

## 2. MATERIALS AND METHODS

Titanium tetrachloride  $\text{TiCl}_4$  (Merck, 99,9%; specific density 1.73 g/cm<sup>3</sup> at 20°C) was cooled to 0°C with. Hydrochloric acid (36,0% aqueous solution) was added to titanium tetrachloride at the stabilized temperature with gaseous hydrogen chloride evaporation.  $\text{TiCl}_4$ : hydrochloric acid final volume ratio was 2:1. Sodium hydrocarbonate aqueous solution was added dropwise to sol of titanium oxychloride  $\text{TiOCl}_2$  up to pH =5.0-5.5 under vigorous stirring. Gel formation was observed during all pH increasing process. The suspension of nanoparticles was kept at 80°C for 3 h with the next washing with distilled water until the absence of  $\text{Na}^+$  and  $\text{Cl}^-$  ions. Precipitated  $\text{TiO}_2$  was dried at the temperature of 150°C, obtained xerogels was marked as S1. The S2 material synthesis process was carried out in analogous was but on the initial stage crystalline dried  $\text{Na}_2\text{SO}_4$  was added directly to titanium tetrachloride with stirring.

Diffraction patterns were obtained with the diffractometer DRON-4-07 equipped with a X-ray tube BSV28 (Cu  $K_\alpha$  radiation, 40 kV, 30 mA). The Bragg-Brentano geometry type and Ni  $K_\beta$  -filter were used. A qualitative analysis was carried out with the use of ICSD structural models. The structural models for anatase and rutile were based on the ICSD ICSD #92363 [31] and ICSD #24780 [32], respectively. Copper powder annealed at vacuum (850 – 900°C for 4 h) with an average grain size of about 50  $\mu\text{m}$  was used as reference sample for the determination of the instrumental peak broadening. Full width at half maximum (FWHM) for a diffraction peak of this reference sample at  $2\theta = 43.38^\circ$  was  $0.129^\circ$ , therefore it permitted to distinguish the phases anatase and brookite. The size of the coherently scattering domains was calculated by the Scherrer equation [33]:  $D = \frac{K\lambda}{\beta \cos\theta}$ , with K is the Scherrer constant ( $K = 0.9$ ),  $\lambda$  is the wavelength (0.15405 nm),  $\beta$  the FWHM (in radians), and  $\theta$  is the peak angular position. As profile shape, we used a combination of Gauss and Cauchy (dominated) functions.

Infrared spectra were recorded at Thermo-Nicolet Nexus 670 FT-IR spectrometer in the region of 4000 – 400  $\text{cm}^{-1}$ . The mixture  $\text{TiO}_2$  / KBr after vibrating milling was pressed into pellets and measured in the transmission mode.

The morphology of sample powders was studied by transmission electron microscopy (TEM) with a 100 kV microscope JEOL JEM-100CX II. The microscopic copper grid covered by a thin transparent carbon film was used as specimen support for TEM investigations.

## 3. RESULTS AND DISCUSSION

The presence of sodium sulfate in the reaction medium abruptly affects on the phase state of the obtained materials (Fig. 1). Material obtained at the absence of  $\text{Na}_2\text{SO}_4$  additive (S1) is a mixture of anatase and rutile with relative contents of  $65 \pm 4$  and  $35 \pm 5$  wt%, respectively. The average size of the coherently scattering domains (CSD) was about 14 nm for anatase and 9 nm for rutile, so the both phases are good crystallized. Meantime part of the material is in the close to amorphous state as evidenced the presence of halo on XRD pattern for  $2\theta = 16-32^\circ$ . Accordingly to synthesis conditions the formation of non-titania phase is unlikely. As the result, material consists of separated part of  $\text{TiO}_2$  with different crystallinity degrees. The specific surface area of S1 sample was about 152  $\text{m}^2 \text{g}^{-1}$ . The material S2 was close to amorphous ultrafine titania with clear structural features of anatase. The halo on XRD pattern is observed in this case too but it's relatively narrowed and shifted to larger  $2\theta$ . The average size of the coherently scattering domains (CSD) was about 4-5 nm (the analysis is complicated by low crystallinity of the material). The specific surface area for S2 sample was increased to 328  $\text{m}^2 \text{g}^{-1}$ .

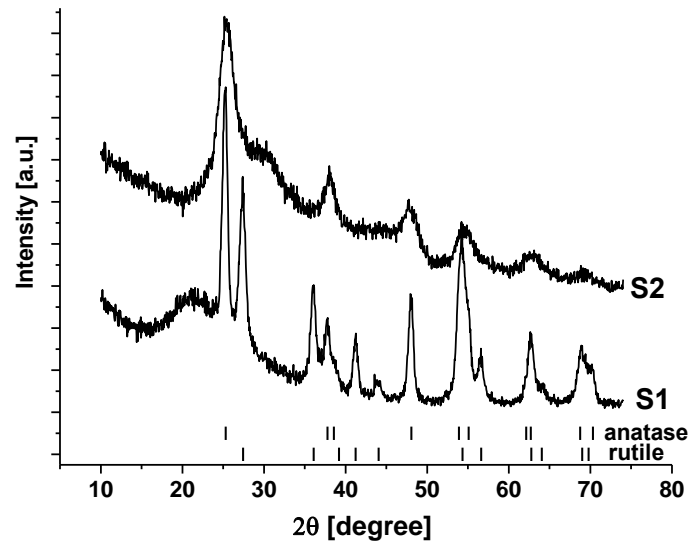
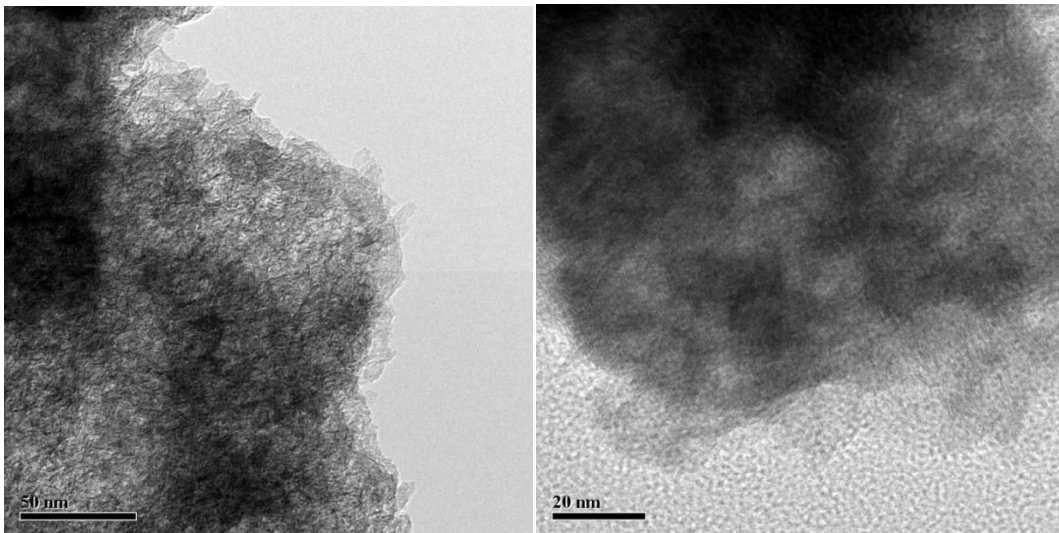


Fig. 1. XRD patterns of S1 and S2 materials.

TEM images of S1 sample (Fig. 2, a) do not allow make the clear conclusions its morphology but on the agglomerates edges material consist of the lamellar-like primary particles with sizes about 10-15 nm. Simultaneously there is no any evidence of crystalline regions boundaries (Fig. 2, b). S2 sample (Fig. 2, c) has bauble-like morphology agglomerates consist of spherical primary particles. HR TEM allows directly observe good crystallinity some of separate grains with arranged atomic layers (Fig. 2, d). Accordingly to direct measurements evidence interplanar distances for crystalline domains vary in narrow range 0.34-0.37 nm (Fig. 3). The obtained interplanar spacing very good corresponds to the (101) plane of anatase (0.352 nm). It indicates the preferred growth direction of coherently scattering domains (crystallites) is [010] crystallography axis. This result correlates to conclusions that the anatase nanocrystals with oxygenated surfaces have developed facets in the (010) direction [11].



a)

b)

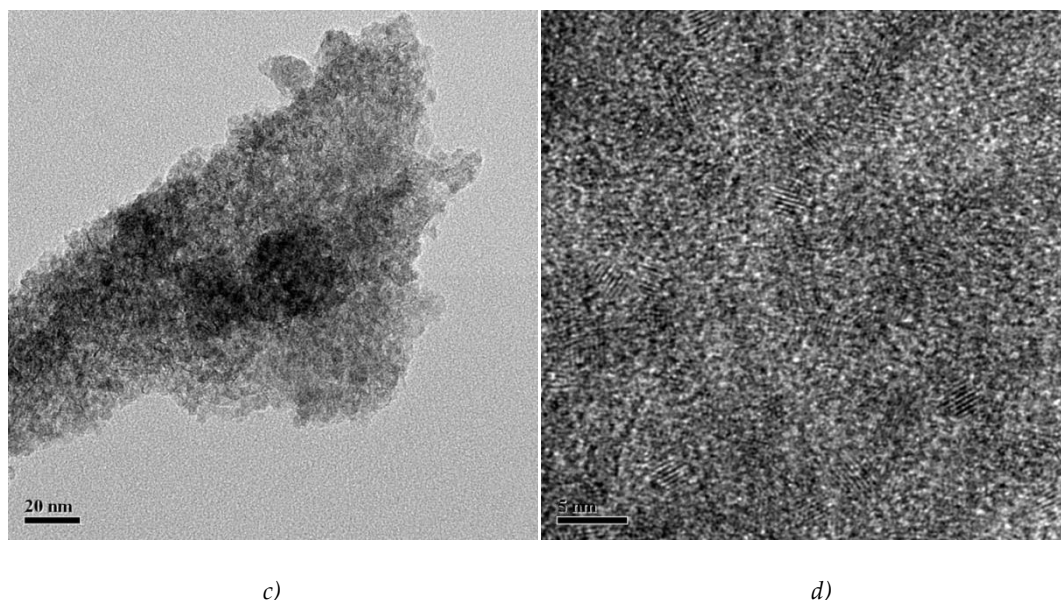


Fig. 2. TEM images of the samples S1 (a,b) and S2 (c,d).

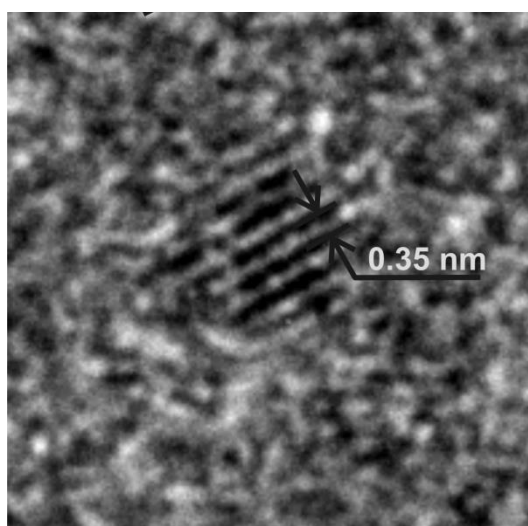


Fig. 3. HR TEM images of S2 material with the fringes from {101} planes.

Additional information about synthesized materials was obtained FT-IR spectroscopy (Fig. 4). The broad absorption region around  $3400\text{ cm}^{-1}$  indicating the presence of chemisorbed OH groups on the titania particles surface ( $\nu$ -OH modes) [12]. The shift of the  $\nu$ -OH bands from typical  $3700\text{--}3600$  to about  $3400\text{ cm}^{-1}$  can be caused the presence of hydrogen bonding [13]. The band around  $1600\text{ cm}^{-1}$  demonstrates the presence of molecularly adsorbed water ( $\delta$ -H<sub>2</sub>O modes) [14]. The higher crystallinity degree for S1 sample causes the formation of relatively more distinct absorption bands in titania characteristic region ( $400\text{--}700\text{ cm}^{-1}$ ) [15].

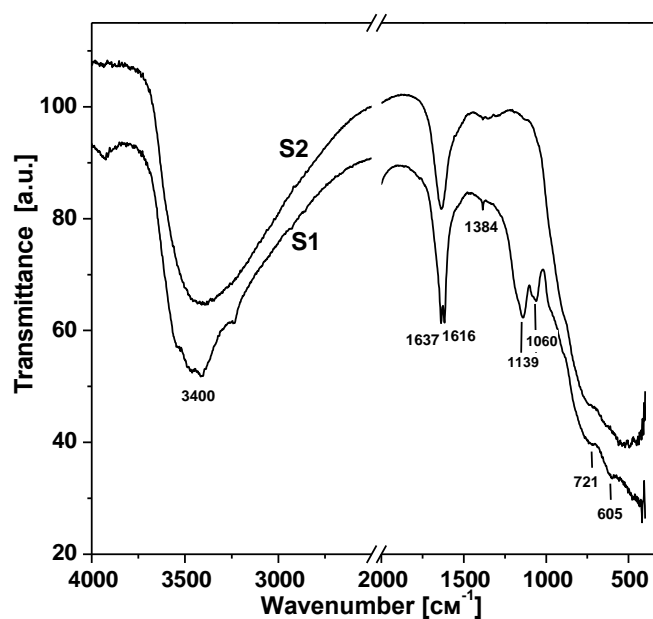


Fig. 4 FTIR spectra of S1 and S2 materials.

The additional absorbance band on the FTIR patterns for S2 materials at 1139 and 1060 corresponding to chemisorbed  $\text{SO}_4^{2-}$  ions [16]. Sharp low intensity band  $1384\text{ cm}^{-1}$  is typical for the metal oxides modified by sulfate ion bands and is assigned to S=O stretching frequency. Meantime S=O-H coordination is unlikely because in this case absorption band will shift in low-frequencies region up to  $1325\text{ cm}^{-1}$ .

There are two different variants of  $\text{SO}_4^{2-}$  immobilization on the titania surface – chelating bidentate complex formation (Fig. 5, a) with coordination to one metal ion through two oxygens or a bridged bidentate complex formation using bonding through two metal ions (Fig. 5, b) [17]; both complexes belong to  $\text{C}_{2v}$  point group.

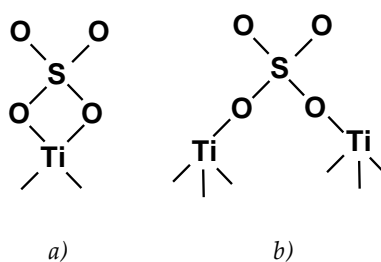


Fig. 5. Possible surface structures for  $\text{SO}_4^{2-}$  chemisorptions on titania: (a) chelating bidentate; (b) bridged bidentate.

The correspondence of  $1139\text{ cm}^{-1}$  band to bidentate sulfate ion coordinated to  $\text{Ti}^{4+}$  ions was fixed in [18].

We can suggest the following model of  $\text{Na}_2\text{SO}_4$  impact on titania nucleation on the stage of olation interaction between primary hydrocomplexes with the taking into account previous work conclusions [19]. Crystal structures of different titania polymorphs – anatase, brookite and rutile – are formed by three-dimensional chains of  $[\text{Ti}^{4+}\text{O}_6]$  octahedrons. Polymorphs differ by mutual position and distortion type of octahedrons. For anatase (space groups  $\text{I}4_1\text{amd}$ ) each octahedron is in contact with 8 neighboring octahedrons (4 sharing edges and 4 sharing vertexes); octahedrons with joint edges align along crystallographic directions  $[100]$  and  $[010]$  and form a broken double chain perpendicular to the  $[001]$  axis. In rutile structure (space group  $\text{P}4_2\text{mnm}$ ) each octahedron is in contact with 10 neighboring

octahedrons (2 sharing edges and 8 sharing vertexes); octahedrons with joint edges align along crystallographic directions [001] (Fig. 6).

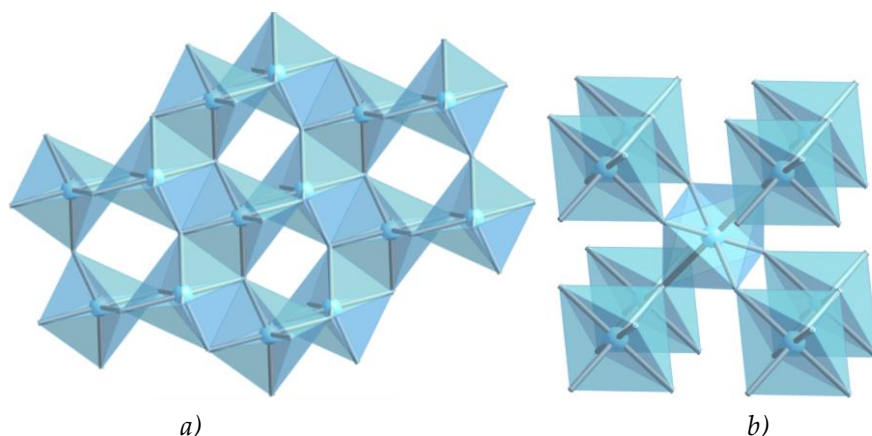


Fig.6.  $[TiO_6]$  coordination octahedrons in the structure of anatase (a) and rutile (b).

The hydrolysis of  $TiCl_4$  leads to  $[Ti(OH_2)_6]^{4+}$  species formation where  $Ti^{4+}$  ions are in the octahedral coordination with the next transformation to  $[Ti(OH)_h(OH_2)_{6-h}]^{(4-h)+}$  monomers as a result of deprotonisation. The hydrolysis ratio  $h$  is a function of pH and determined by partial charge theory [20]. In these monomers  $OH^-$  groups have thermodynamic advantages of the location in the octahedrons equatorial planes, and  $H_2O$  molecules primarily occupy the "vertex" position [21]. The hydrolysis products are  $[Ti(OH)(OH_2)_5]^{3+}$  and  $[Ti(OH)_2(OH_2)_4]^{2+}$  monomers when pH of reaction medium is close to 1. If  $pH = 3$ , the  $[Ti(OH)_2(OH_2)_4]^{2+}$  and  $[Ti(OH)_3(OH_2)_3]^+$  complexes coexist in solution. At pH being equal to 4 the hydrolysis leads to the formation of the  $[Ti(OH)_3(OH_2)_3]^+$  complexes and in the range of pH 6 - 8 the  $[Ti(OH)_4(OH_2)_2]^0$  monomers are formed. The possibility of titania polymorph formation is defined by spatial organization of  $[Ti(OH)_h(OH_2)_{6-h}]^{(4-h)+}$  primary monomers.  $[Ti(OH)_4(OH_2)_2]^0$  monomers in which OH groups occupying octahedrons equatorial planes with  $H_2O$  molecules in the vertexes have been formed in neutral or alkaline mediums. Dimers are formed as a result of olation reaction between the two primary monomers for which the coordination octahedrons have a common edge outside the octahedron equatorial plane. After further polycondensation the zigzag-like or spiral chain of  $[Ti_n(OH)_{4n}(OH_2)_2]^0$  polyhedrons are formed and the conditions for the anatase phase nucleation are created. The  $[Ti_{mn}O_{mn}(OH)_{2mn}(OH_2)_{2m}]^0$  polymer is formed resulting from  $m$  linear structures of  $[Ti_n(OH)_{4n}(OH_2)_2]^0$  olation interaction. Nucleation of anatase phase is the result of octahedral merger by lateral planes of faces (Fig. 6,a). At the same time the hydronium ions of the reaction medium interact with OH groups in the octahedrons equatorial plane. If the hydronium ions concentration in the reaction medium grows,  $[Ti(OH)_h(OH_2)_{6-h}]^{(4-h)+}$  monomers will be formed under  $h < 2$  condition. Olation interaction between them leads to the polymer chains formation where monomers are linked by joint edges in octahedrons equatorial planes thus defining the precondition for rutile phase nucleation. The presence of  $SO_4^{2-}$  groups in the reaction medium will cause chelating bidentate complexes formation in the octahedrons equatorial planes (Fig.7,a). As a result the olation interaction between monomers with a common edge outside the octahedron equatorial plane is prevailing. In these conditions polycondensation the zigzag-like or spiral chain of  $[Ti_n(OH)_{4n}(OH_2)_2]^0$  polyhedrons are formed and the conditions for the anatase phase nucleation are created (Fig. 7, b).

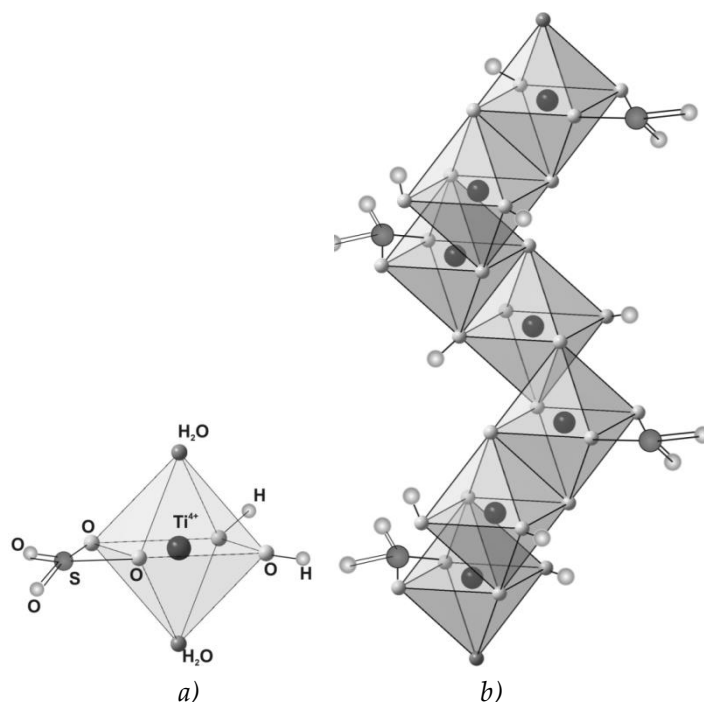


Fig. 7. A scheme of separate  $[\text{Ti}(\text{OH})_2(\text{OH})_2\text{SO}_4]^0$  monomer (a) and possible formation of oligomeric chains with anatase phases nucleation (b).

#### 4. CONCLUSIONS

An effect of  $\text{SO}_4^{2-}$  sulphate anions on the titania nucleation during hydrolysis of titanium tetrachloride was analyzed. It is assumed that the presence  $\text{SO}_4^{2-}$  leads to chelating bidentate complex formation on the stage of primary monomers  $[\text{Ti}(\text{OH})_n(\text{OH})_{6-n}]^{(4-n)+}$  oligation interaction. Sulphate anions bonding to titanium ion through two oxygens in the octahedrons equatorial planes causes the predominant oligation between monomers with a common edge outside the octahedron equatorial plane. As a result of polycondensation the zigzag-like of  $[\text{Ti}_n(\text{OH})_{4n}(\text{OH})_2]^0$  polyhedrons are formed and the conditions for the anatase phase nucleation are performed.

#### REFERENCES

- [1] Yamashita H., Harada M., Misaka J., Takeuchi M., Neppolian B., Anpo M. Photocatalytic degradation of organic compounds diluted in water using visible light-responsive metal ion-implanted  $\text{TiO}_2$  catalysts: Fe ion-implanted  $\text{TiO}_2$ . *Catalysis Today*, **84** (3) (2003), 191-196. doi:10.1016/S0920-5861(03)00273-6
- [2] Kazuhito H., Irie H., Fujishima A.  $\text{TiO}_2$  photocatalysis: a historical overview and future prospects. *Japanese journal of applied physics*, **44** (12) (2005), 8269-8285. doi: 10.1143/JJAP.44.8269
- [3] Agrios A.G., Pierre P. State of the art and perspectives on materials and applications of photocatalysis over  $\text{TiO}_2$ . *Journal of Applied Electrochemistry*, **35** (7) (2005), 655-663. doi:10.1007/s10800-005-1627-6
- [4] Bao S.J., Li C.M., Zang J.F., Cui X.Q., Qiao Y., Guo J. New nanostructured  $\text{TiO}_2$  for direct electrochemistry and glucose sensor applications. *Advanced Functional Materials*, **18** (4) (2008), 591-599. doi:10.1002/adfm.200700728
- [5] O'regan B., Grfitzeli M. A low-cost, high-efficiency solar cell based on dye-sensitized. *Nature*, **353** (6346) (1991), 737-740. doi:10.1038/353737a0

- [6] Xu N., Shi Z., Fan Y., Dong J., Shi J., Hu M.Z.C. Effects of particle size of TiO<sub>2</sub> on photocatalytic degradation of methylene blue in aqueous suspensions. *Industrial & Engineering Chemistry Research*, **38** (2) (1999), 373-379. doi:10.1021/ie980378u
- [7] Testino A., Bellobono I.R., Buscaglia V., Canevali C., D'Arienzo M., Polizzi S., Morazzoni F. Optimizing the photocatalytic properties of hydrothermal TiO<sub>2</sub> by the control of phase composition and particle morphology. A systematic approach. *Journal of the American Chemical Society*, **129** (12) (2007), 3564-3575. doi:10.1021/ja067050+
- [8] Macwan D.P., Dave P.N., Chaturvedi S. A review on nano-TiO<sub>2</sub> sol-gel type syntheses and its applications. *Journal of Materials Science*, **46** (11) (2011), 3669-3686. doi:10.1007/s10853-011-5378-y
- [9] Gupta S.M., Tripathi M. A review on the synthesis of TiO<sub>2</sub> nanoparticles by solution route. *Central European Journal of Chemistry*, **10** (2) (2012), 279-294. doi: 10.2478/s11532-011-0155-y
- [10] Yin H., Wada Y., Kitamura T., Kambe S., Murasawa S., Mori H., Yanagida S. Hydrothermal synthesis of nanosized anatase and rutile TiO<sub>2</sub> using amorphous phase TiO<sub>2</sub>. *Journal of Materials Chemistry*, **11** (6) (2011), 1694-1703. doi: 10.1039/B008974P
- [11] Barnard A.S., Curtiss L.A. Prediction of TiO<sub>2</sub> nanoparticle phase and shape transitions controlled by surface chemistry. *Nano letters*, **5** (7) (2005), 1261-1266. doi: 10.1021/nl050355m
- [12] Sivakumar S., Pillai P.K., Mukundan P., Warriar K.G.K. Sol-gel synthesis of nanosized anatase from titanyl sulfate. *Materials letters*, **57** (2) (2002), 330-335. doi:10.1016/S0167-577X(02)00786-3
- [13] Gutierrez-Alejandre A., Gonzalez-Cruz M., Trombetta M., Busca G., Ramirez J. Characterization of alumina-titania mixed oxide supports: Part II: Al<sub>2</sub>O<sub>3</sub>-based supports. *Microporous and mesoporous materials*, **23** (5) (1998), 265-275. doi:10.1016/S1387-1811(98)00121-8
- [14] Karuppuchamy S., Jeong J.M. Synthesis of nano-particles of TiO<sub>2</sub> by simple aqueous route. *Journal of Oleo Science*, **55** (5) (2006), 263-266. doi: 10.5650/jos.55.263
- [15] Djaoued Y., Robichaud J., Bruning R. The effect of polyethylene glycol on the crystallization and phase transitions of nanocrystalline TiO<sub>2</sub> thin films. *Materials Science-Poland*, **23** (1) (2005), 15-27.
- [16] Yamaguchi T., Jin T., Ishida T., Tanabe K. Structural identification of acid sites of sulfur-promoted solid super acid and construction of its structure on silica support. *Materials chemistry and physics*, **17**(1-2) (1987), 3-19. doi:10.1016/0254-0584(87)90045-9
- [17] Raj K.J.A., Viswanathan B. Single-step synthesis and structural study of mesoporous sulfated titania nanopowder by a controlled hydrolysis process. *ACS applied materials & interfaces*, **1** (11) (2009), 2462-2469. doi: 10.1021/am900437u
- [18] Sohn J.R., Lee S.H., Cheon P.W., Kim, H.W. Acidic Properties and Catalytic Activity of Titanium Sulfate Supported on TiO<sub>2</sub>. *Bulletin-korean chemical society*, **25** (5) (2004), 657-664.
- [19] Kotsyubynsky V.O., Myronyuk I.F., Myronyuk L.I., Chelyadyn V.L., Mizilevska M.H., Hrubciak A.B., Tadeush O.K., Nizamutdinov F.M. The effect of pH on the nucleation of titania by hydrolysis of TiCl<sub>4</sub>. *Materialwissenschaft und werkstofftechnik*, **47** (2-3) (2016), 288-294. doi: 10.1002/mawe.201600491
- [20] Henry M., Jolivet J.P., Livage J. *Aqueous chemistry of metal cations: hydrolysis, condensation and complexation*. In: Chemistry, Spectroscopy and Applications of Sol-Gel Glasses, **77**, 1992, 153-206. doi: 10.1007/BFb0036968
- [21] Kumar S.G., Rao K.K. Polymorphic phase transition among the titania crystal structures using a solution-based approach: from precursor chemistry to nucleation process. *Nanoscale*, **6** (20) (2014), 11574-11632. doi: 10.1039/C4NR01657B

**Address:** V.O. Kotsyubynsky, I.F. Myronyuk, B.K. Ostafiychuk, A.B. Hrubciak, I.I. Hryhoruk, Vasyl Stefanyk Precarpathian National University, 57, Shevchenko Str., Ivano – Frankivsk, 76018, Ukraine;  
V.L. Chelyadyn, Institute of Materials Science, I.M. Frantsevich, 3, Academic Krzhizhanovskii Str., Kyiv, 03680, Ukraine.

**E-mail:** v\_kotsyubynsky@mail.ru; ivan.myroniuk@pu.if.ua; bo@pu.if.ua; ira.hryhoruk@gmail.com; VICHel@tut.by; hrubyak\_andrii@ukr.net.

**Received:** 28.01.2016; **revised:** 12.04.2016.



Коцюбинський В.О., Миронюк І.Ф., Остафійчук Б.К., Челядин В.Л., Груб'як А.Б., Григоруk І.І. Вплив сульфат аніонів  $\text{SO}_4^{2-}$  на процес нуклеації титану. *Журнал Прикарпатського університету імені Василя Стефаника*, 3 (1) (2016), 29–37.

Запропоновано та експериментально апробовано феноменологічну модель впливу сульфат аніонів  $\text{SO}_4^{2-}$  на нуклеацію титану в процесі гідролізу тетраклориду титану. Сульфат аніони із первинних комплексів  $[\text{Ti}(\text{OH})_h(\text{OH}_2)_{6-h}]^{(4-h)+}$  утворюють бідентантні хелатні комплекси, впливають на процес протікання оляційних взаємодій та формування зародків фази анатазу.

**Ключові слова:** гідроліз, поліконденсація, енуклеація, анатаз, сульфат аніони.